Arabian Journal of Geosciences (2021) 14: 750
https://doi.org/10.1007/s12517-021-07080-9

ORIGINAL PAPER

Depositional facies and diagenesis of the Lianglitage Formation in northwestern Tazhong Uplift, Tarim Basin, China: implications for the genesis of ultra-deep limestone reservoir

Da Gao [1,2] · Changsong Lin [3] · Lili Huang [4] · Mingyi Hu [1,2] · Ping Ren [5] · Chunyan Sun [5] · Yuru Zhao [1,2]

Received: 7 January 2021 / Accepted: 5 April 2021 / Published online: 20 April 2021

Abstract

The limestone reservoir beds of Late Ordovician Lianglitage Formation are preserved in northwestern Tazhong Uplift of the Tarim Basin with buried depth exceeding 6000 m. The origin of the ultra-deep limestone reservoir is still controversial, which restricts the further hydrocarbon exploration. In order to clarify the main controlling factors of reservoirs, we carried out the study of sedimentary facies, diagenesis, and reservoir characteristics based on seismic, well logging, and core data. The Lianglitage Formation in northwestern Tazhong Uplift is mainly composed of nine lithofacies that are deposited from platform margin reef-shoal, platform-interior shoal, and restricted lagoon to tidal flat environments. The Lianglitage Formation has experienced syndepositional submarine diagenesis, penecontemporaneous diagenesis, and burial diagenesis, and consequently the reservoir space in the formation mainly includes fractures and dissolution vugs and caves. Reef and shoal deposits are the material basis of favorable reservoirs, and the favorable reservoirs have been mostly improved by the dissolution of meteoric water in penecontemporaneous diagenesis. In the burial stage, the early-formed porosity was destroyed by cementation to some extent, but the fractures and associated vugs formed in the late Ordovician and Silurian-Devonian played an important role in the improvement of the reservoir. The results are of great significance to the prediction of deep carbonate reservoirs and the hydrocarbon exploration in basins of western China. Favorable facies, early-stage improvement by meteoric water, and tectonic fracture are key to the formation of high-quality large-scale deep limestone reservoirs.

Keywords Deep-burial · Carbonate reservoir · Depositional facies · Diagenesis · Lianglitage Formation · Tarim Basin

Introduction

Hydrocarbon exploration of the petroliferous basins in western China have been advancing to deep-burial carbonate reservoirs from Sinian to Ordovician systems. In carbonate succession, the reservoir beds with burial depth greater than 4500 m is defined as deep reservoir, and the reservoir beds with burial depth greater than 6000 m is defined as ultra-deep reservoir, which has been widely accepted in China (He et al. 2016; Ma et al. 2020). A large number of studies show that the high-quality deep/ultra-deep carbonate reservoirs are mainly related to three important factors, which are favorable sedimentary conditions, tectonism and fracture development, and fluid-rock interaction (Ma et al. 2019), but the main controlling factors vary due to different geological conditions. Exploring the main controlling factors of the formation of deep and ultra-deep carbonate reservoirs is an important prerequisite for further predicting the distribution of high-quality

Responsible Editor: Attila Ciner

✉ Da Gao
gaoda18@gmail.com

[1] Key Laboratory of Exploration Technologies for Oil and Gas Resources (Yangtze University), Ministry of Education, Wuhan 430100, China

[2] School of Geosciences, Yangtze University, Wuhan 430100, China

[3] School of Ocean Sciences, China University of Geosciences, Beijing 100083, China

[4] PetroChina Hangzhou Research Institute of Geology, Hangzhou 310023, China

[5] Research Institute of Petroleum Exploration and Production, Tarim Oilfield Company, PetroChina, Korla 841000, China

reservoirs. For example, the Sinian to Cambrian dolomite reservoirs (4500~5390m) in the Anyue gas field of the Sichuan Basin is mainly affected by favorable depositional facies and karstification (Zou et al. 2014), while the Cambrian-Ordovician carbonate reservoirs in the Tahe oil field of the Tarim Basin is mainly controlled by tectonism and supergene karstification (Ma et al. 2013). The Permian-Triassic carbonate reservoir (6327~7013 m) in the Yuanba gas field of the Sichuan Basin are mainly affected by depositional facies, dolomitization, and karstification (Ma et al. 2014), while the Ordovician carbonate reservoirs (7200~8500 m) in the Shunbei oil and gas field of the Tarim Basin is mainly affected by fault-karstification (Jiao 2018).

The Lianglitage Formation is characterized by the development of Ordovician reef and shoal deposits in the Tazhong Uplift, and the distribution of reef-shoal facies were mainly controlled by Tazhong No.1 fault located in the edge of Tazhong Uplift and spreading in NE-SW direction (Fig. 1a) (Gao et al. 2014; Lin et al. 2009). Previous studies are mostly based on the wells in the eastern part of Tazhong area where the Lianglitage Formation are buried at 4000~5000 m. It is generally considered that early karstification is the most important factor for the reef-shoal reservoirs and fractures formed by multiple-stage tectonic movements further improve reservoir quality (Gao et al. 2013; Liu et al. 2010; Lü et al. 2008; Qu et al. 2013; Zhao et al. 2007; Zhou et al. 2008). As for the northwestern Tazhong Uplift where the buried depth of the Lianglitage Formation is greater than 6000 m, favorable reservoirs and condensate gas accumulation with industrial exploitation value have also found (Lü et al. 2012). However, there is still no consistent understanding of the genetic process of the ultra-deep reservoir. Most researchers support that the reef and shoal of the Lianglitage Formation is the material basis of favorable reservoirs (Han et al. 2011; Wei et al. 2020; Yan et al. 2019; Zhu et al. 2010; Zuo et al. 2014), and the fractures formed by tectonism play an

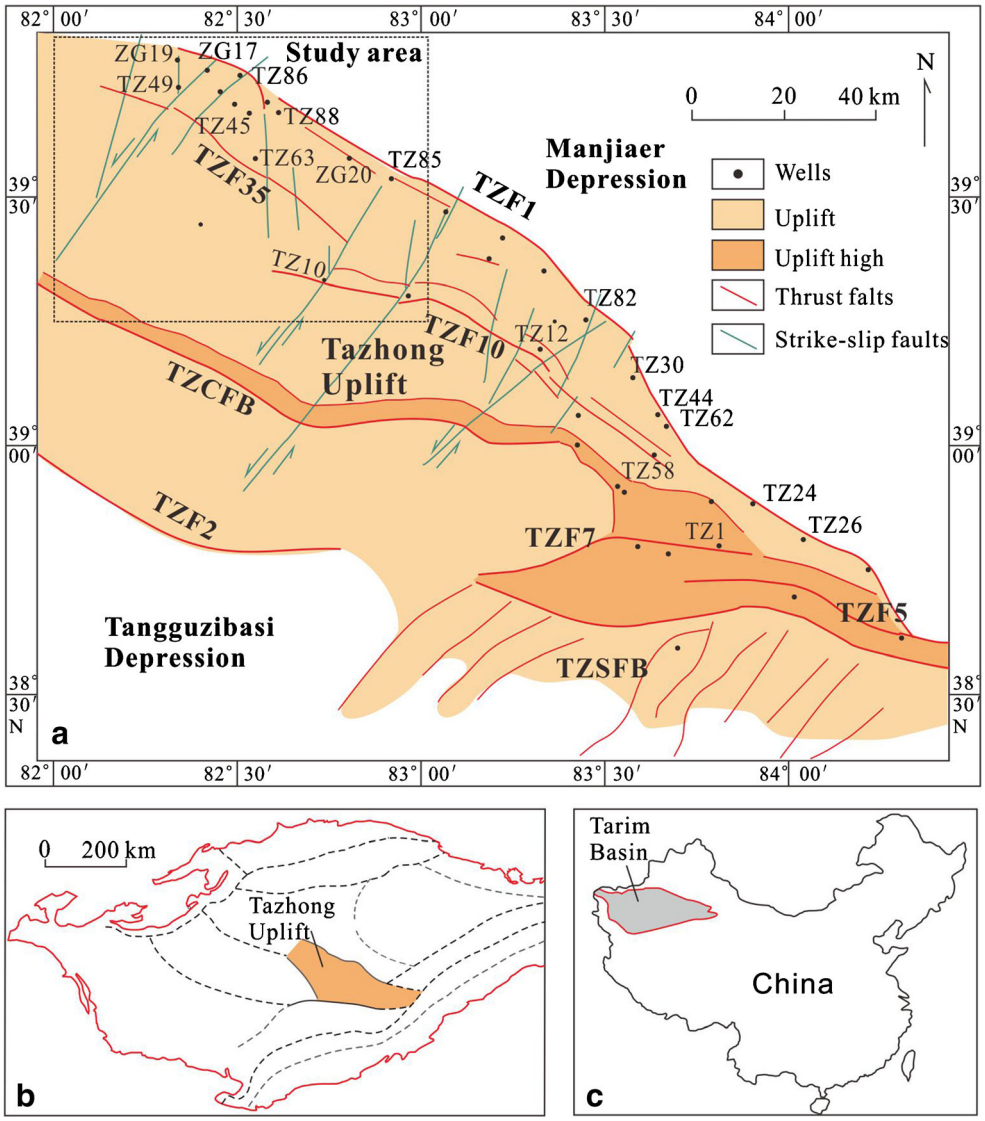

Fig. 1 Location and structural map of the Tazhong Uplift. The distribution of faults in the Tazhong Uplift (**a**) modified from Wu et al. (2012). TZF1, Tazhong Fault No.1; TZF2, Tazhong Fault No.2; TZF5, Tazhong Fault No.5; TZF7, Tazhong Fault No.7; TZF10, Tazhong Fault No.10; TZF35, Tazhong Fault No.35; TZCFB, Tazhong Central Fault Belt; TZSFB, Tazhong South Fault Belt

important role in reservoir improvement (Qiu et al. 2017; Zhang et al. 2016a, b). Additionally, there are different understandings about the type of karstification. Some researchers hold that early karstification is the most important factor (Qian et al. 2008, 2013; Wei et al. 2020), while others considered that deep hydrothermal activity during burial stage is the most beneficial to the karst reservoirs (Deng et al. 2018; Han et al. 2011; Lü et al. 2005; Wang and Lü 2004; Wang et al. 2004). The unconsolidated understanding of reservoir genesis restricts reservoir prediction and oil and gas exploration.

The purpose of this paper is to clarify the main controlling factors of the formation of ultra-deep reef-shoal reservoirs in northwestern Tazhong Uplift based on the study of sedimentation and diagenesis. The research results provide support for the distribution and prediction of reservoirs in the region and can also shed light on the genesis of deep-burial limestone reservoirs.

Geological setting

The Tazhong Uplift is one of the most important hydrocarbon-bearing tectonic belts at the center of the Tarim Basin, Northwest China (Fig. 1) (Yang et al. 2014). During the Paleozoic, the Tazhong Uplift experienced a series of tectonic events (Jia 1997; Lin et al. 2012a). The paleogeomorphic patterns at different stages significantly influenced the distribution of depositional systems (Lin et al. 2009; Liu et al. 2012). After intense uplift during the Middle Ordovician, the northwestern part of the Tazhong Uplift was significantly higher than the southeastern part (Peng et al. 2009). During the early stage of the Late Ordovician, a large carbonate platform formed on top of this uplift, and the platform margin is largely controlled by the Tazhong Fault No.1 which serves as the northeastern boundary of the uplift (Peng et al. 2009; Wu et al. 2012).

The Late Ordovician carbonate platform margin has different facies associations along the Tazhong Fault No.1 (Chen et al. 2009; Gao et al. 2014; Liu et al. 2012). The southeastern part of the platform margin is mainly composed of thick reef and shoal deposits showing a vertical accretion trend across a narrow range. The platform margin facies belt at the central part is wide in range and characterized by progradation, while the platform margin at the northwestern part displays a retrograde ramp (Lin et al. 2012a). Shallow-water carbonate deposition was terminated by a rapid marine transgression during the late stage of the Late Ordovician, causing deepwater siliciclastic shelf deposits to overlay the carbonate strata in the uplift (Gao et al. 2014). At the end of the Ordovician, the southeastern part of the Tazhong Uplift experienced a significant uplift that resulted in the erosion of a large portion of the Upper Ordovician, while the northwestern area of the Tazhong Uplift subsided (Chen et al. 2009; Lin et al. 2012a). At present, the Lianglitage Formation is about 4000- to 5000-m deep at the southeastern part and up to 6000- to 7000-m deep at the northeastern part of the Tazhong Uplift.

The Lianglitage Formation consists of mainly shallow marine carbonate deposits and a small amount of terrigenous clay in the lower and upper parts (Fig. 2). Based on clay content, this formation is divided into three members (Lin et al. 2009; Yang et al. 2000). Three depositional sequences (SQ1, SQ2, and SQ3) have also been identified in both seismic and well data (Fig. 2). The main reservoir space of the Lianglitage Formation includes pores, vugs, and fractures. The reservoir beds with fracture-pore composite porosity are the best in reservoir property, and they mainly occur at the upper part of the grainstone member (Liu et al. 2009). Along the platform margin zone, the main types of reservoir porosity vary with the change of depositional facies and the structural patterns of TZF1 (Fig. 1). The reservoir porosity is dominated by fractures and pores in TZ82-TZ24 area and is mainly characterized by pores and small caves in TZ62 area (Gao et al. 2013; Liu et al. 2009). The types of porosity in the Lianglitage Formation at the northwest of the Tazhong Uplift include pores, fractures, and pores (Wei et al. 2020).

Materials and methods

Data from 3-D seismic profiles, logs from 12 wells, and analysis of 155-m core from six wells are integrated in this study. The petrography of the Lianglitage Formation is described from the cores and thin sections, and all the thin sections were examined using transmitted light optical microscopy and cathodoluminescence.

The classification of carbonate rocks follows the nomenclature of Dunham (1962) and Embry and Klovan (1971). Lithofacies classification is largely adopted from Gao et al. (2014), and sequence stratigraphy of the Lianglitage Formation is adopted from Yang et al. (2010) and Gao et al. (2014). Diagenetic features were mainly distinguished by shape and the cathodoluminescence of the cements in the thin sections. The diagenetic environments and diagenetic stages were interpreted in accordance with Scholle and Ulmer-Scholle (2003) and Moore (2001).

Facies analysis

Lithofacies and facies associations

The Lianglitage Formation in the northwest of Tazhong Uplift is mainly composed of nine types of lithofacies (Fig. 3, Table 1). The description and sedimentary condition interpretation of those lithofacies are shown in Table 1. The nine lithofacies types can be grouped into three types of facies

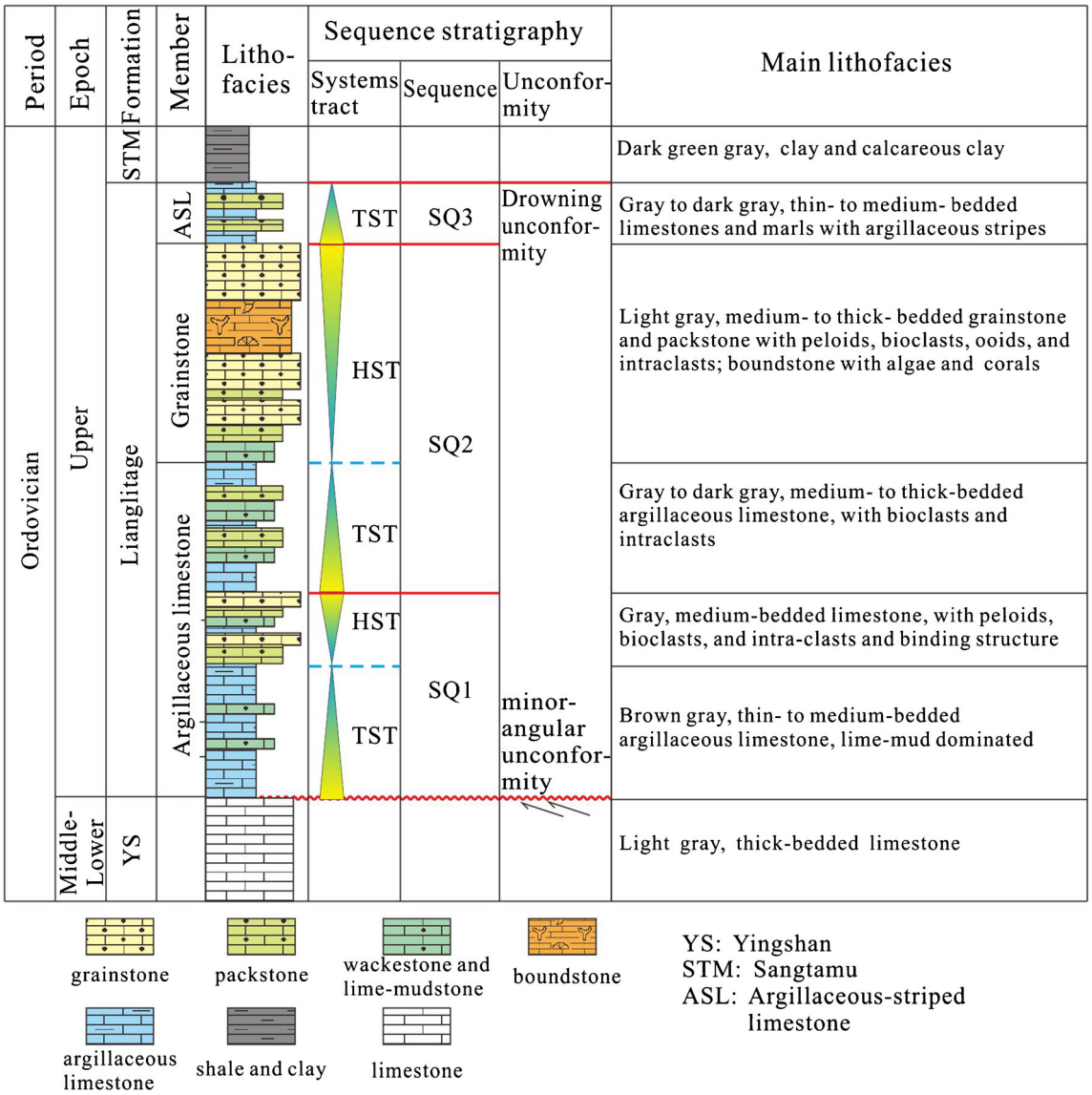

Fig. 2 Sequence stratigraphy and the main lithofacies of the Lianglitage Formation, modified from Gao et al. (2013)

association, which are interpreted to be deposited in platform margin reef and shoal, platform-interior sand shoal, and restricted lagoon-tidal flat.

Platform margin reef and shoal facies association

Description This facies association consists of four lithofacies types (Lf1~Lf4, Fig. 3a–f). In some lithofacies, ooids and well-rounded intraclasts are well sorted, while in some lithofacies, the distribution of grain size has two peaks. Bryozoan, coral, and bivalve are common in skeleton grains, and their outer edges are little to moderate abraded. This type of facies association is very common at the middle-upper part of the Lianglitage Formation in wells near Tazhong No.1 fault (such as TZ85, TZ86, and TZ88, Fig. 4). It developed continuously in the vertical direction, occupying most of the strata and occasionally interrupted by lagoon deposits (Fig. 4). In well logging, GR logging has low value and weakly jagged curve pattern, while resistivity logging has medium-low value and moderate-jagged pattern (Fig. 4).

Interpretation Well-sorted ooids which have intraclasts as cores (Fig. 3a, b) indicate a constantly agitated water condition that was influence by wave and tide. Coarse ellipsoidal ooids and intraclasts are largely arranged in similar direction (Fig. 3c), indicating they were deposited in tidal channel environment. The fossils include bryozoan, coral, bivalve, and green algae that are commonly found in well-circulated shallow marine. The skeleton grains are mostly larger in size than non-skeleton grains and have moderate to low degree of abrasion, indicating they underwent a short transportation (Fig. 3e, f). These characteristics generally reflect they were deposited in the environment of reefs and shoals located at the platform margin.

Table 1 Description and interpretation of lithofacies and facies associations of the Lianglitage Formation, NW Tazhong Uplift

Facies association	Lithofacies type	Non-skeletal components	Main fossils	Sedimentary structures	Hydrodynamic condition	Depositional environment
FA1	Lf1: Ooid grainstone (Fig. 3a)	Well-sorted and tightly packed ooids with round shape and multiple concentric layers, usually 0.5~1 mm in diameter	Green algae fragments	Massive	High energy, intense waves and tides, above fair weather wave base	Ooid bar, platform margin
	Lf2: Ooid and peloid grainstone (Fig. 3b, c)	Most ooids are large (1~2 mm) and elliptical in shape, having thin cortical coatings and large nuclei which are usually peloids and aggregated grains. Peloids are sub-rounded in shape and usually 0.2~0.5 mm in size	Calcareous algae and shell fragments of bivalves and gastropods; shells generally have micritic envelopes	Cross bedding	High energy, tide dominated, above fair weather wave base	Tidal channel between ooid bar, platform margin
	Lf3: Bioclast and peloid packstone and grainstone (Fig. 3d, e)	Aggregated grains are large (1~5 mm) and bad sorting	Large elongated shell fragments of bivalves, well-preserved calcareous algae (*Codiales*), and corals (*Titradium)*	Massive	Moderated to high energy, near fair weather wave base	Back reef, open platform, and platform margin
	Lf4: Algae and coral boundstone (Fig. 3f)	Pellet, small peloids, and micrite are binding together between and around large body fossils	Large corals (*Titradium*) (2~8 mm) are the dominant fossils; algae include *Anthracoporella*, *Solenopora*, and cryptic algae	Binding and baffling structure	Moderate to low energy, below fair weather wave base	Reef core, platform, and platform margin
FA2	Lf5: Peloid grainstone (Fig. 3g, h)	Rounded to sub-rounded, moderated- to bad-sorted peloid are dominated; large aggregated grains and micritic ooids also occur	A small proportion of well-preserved calcareous algae	Massive	Moderate energy, near fair weather wave base	Open platform
	Lf6: Bioclast and peloid wackestone to packstone (Fig. 3i)	Rounded to sub-rounded peloids are the main grains	Well-preserved ostracods, gastropods, and bryozoans; thin and small fragments of bivalves	Massive	Low energy, below fair weather wave base, deep subtidal zone	Lagoon, open platform
FA3	Lf7: Pellet packstone to grainstone (Fig. 3j)	Most grains are dark-colored, rounded- or elliptical-shaped pellets (0.1~0.3 mm); some small micritic ooids	Body fossils are scarce	Massive	Moderate energy, near fair weather wave base	Lagoon, restricted platform
	Lf8: Peloid bindstone (Fig. 3k)	Pellet, small peloids, and micrite are binding together	Body fossils are scarce	Thin bedding, and bird's-eye/fenestra structures	Low energy, tide dominated	Intertidal flat
	Lf9: Thin-bedded mudstone (Fig. 3l)	Micrite dominated	Body fossils are scarce	Shrinkage fissures and bird's-eye structures	Low energy, tide dominated	Inter- to supra- tidal flat

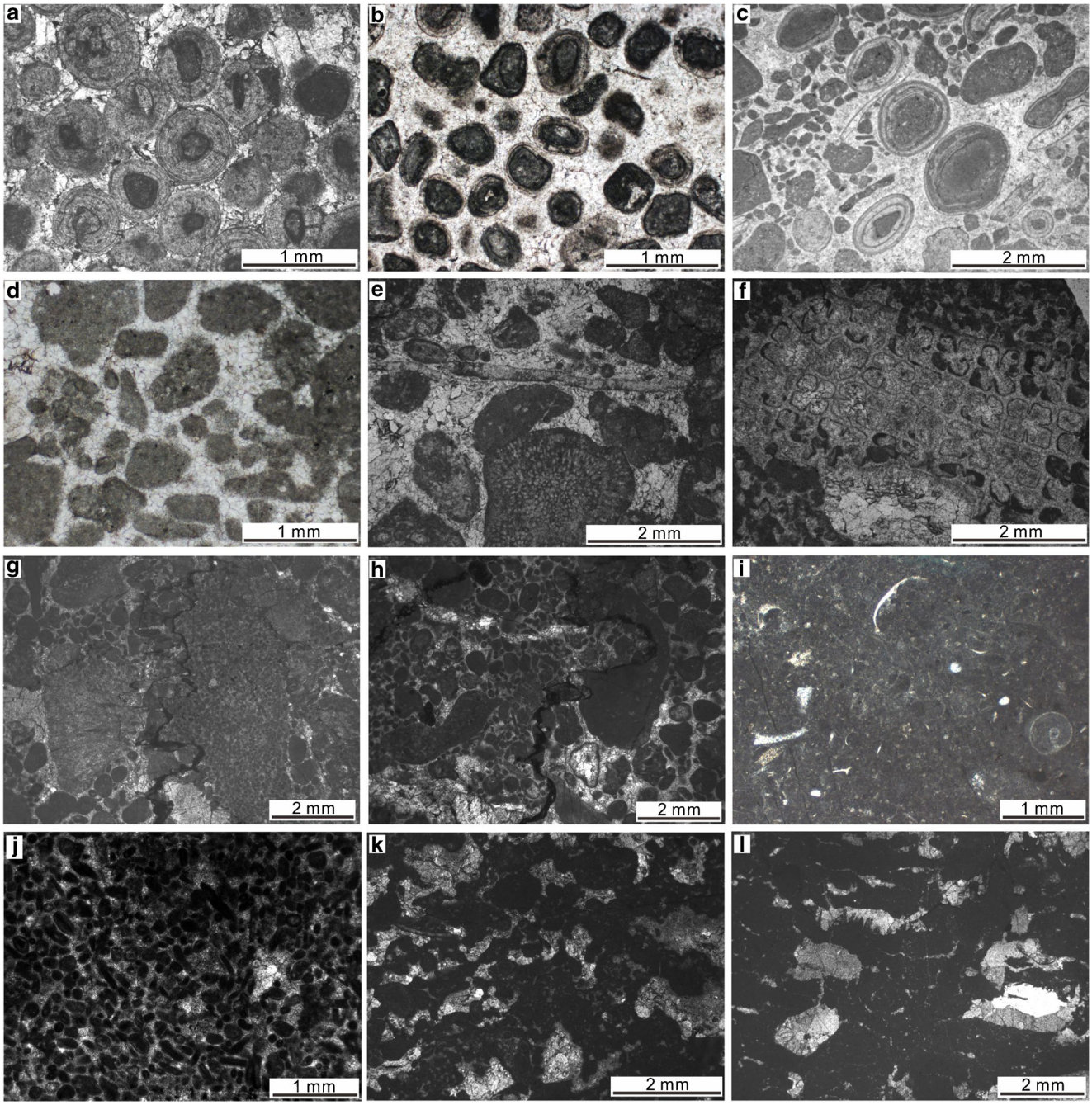

Fig. 3 Photomicrographs of the main lithofacies types in the Lianglitage Formation, NW Tazhong Uplift. **a** Ooid grainstone (Lf1), TZ85, 6535.2 m; **b** ooid and peloid grainstone (Lf2), TZ86, 6274.1 m; **c** ooid and peloid grainstone (Lf2), TZ85, 6442.3 m; **d** aggregated grain packstone (Lf3), TZ86, 6275.2 m; **e** bioclast and aggregated grain packstone (Lf3), TZ85, 6367.4 m; **f** algae and coral boundstone (Lf4), TZ85, 6368.2 m; **g** peloid grainstone (Lf5), TZ49, 6187.3 m; **h** peloid grainstone (Lf5), TZ49, 6189.5 m; **i** bioclast and peloid wackestone to packstone (Lf6), TZ49, 6180.8 m; **j** pellet grainstone (Lf7), TZ49, 6191.6 m; **k** peloid bindstone with fenestra pores (Lf8), TZ49, 6124.0 m; **l** mudstone with shrinkage fissures and bird's-eye structures (Lf9), TZ49, 6128.5 m

Platform-interior sand shoal facies association

Description The facies association consists of Lf5 and Lf6 (Fig. 3g–i). These lithofacies are composed of poorly sorted peloids, skeletal grains, and lime mud and contain moderate amounts of gastropods, bivalves, green algae, and bryozoan fossil, which are usually well preserved (Fig. 3g–i). Vertically, Lf6 usually transits upward to Lf5. This kind of facies association is mainly distributed in the wells located in the west of Tazhong No.1 fault zone, such as TZ49 and TZ45 (Fig. 4). It is mainly distributed dispersedly in the middle and upper parts of the Lianglitage Formation and commonly develops

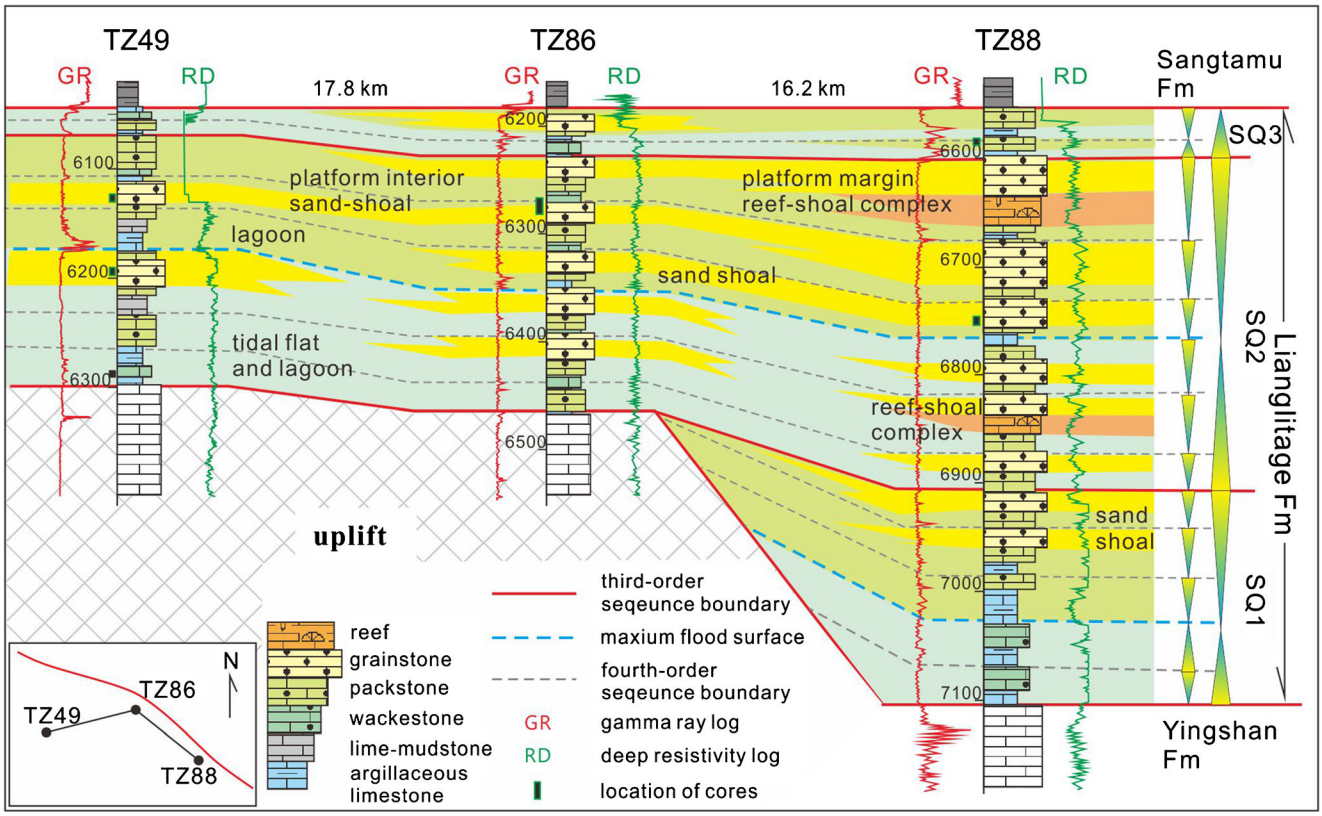

Fig. 4 Facies distribution in the sequence stratigraphy framework of the Lianglitage Formation, northwest Tazhong area

alternately with lagoon and tidal flat deposit. Thus, the facies association vertically occupies just a small proportion (less than 1/4) of the total thickness of the formation. The logging curve patterns of this facies association is similar with that of platform margin reef and shoal facies association, except that the former has smaller thickness and frequently alternates with high-value GR section (Fig. 4).

Interpretation Fossils mainly composed of green algae and mollusks (Fig. 3g–i) indicate an open and photic environment. The grains are poorly sorted and accompanied by a certain amount of lime mud, indicating moderate to weak hydrodynamic force. The sedimentary environment of this facies association is interpreted to be a shoal environment that was intermittently influenced by moderate hydrodynamic force at an open platform.

Restricted lagoon-tidal flat facies association

Description This type of facies association is composed of Lf7~Lf9 (Fig. 3j–l) and contains peloids and very few biological fossils. Horizontal beddings, fenestra structures, and binding structures are common in this facies association, and clay is often contained in matrix-rich lithofacies. The facies association is widely distributed in the drilling wells located in the west of No.1 fault and develops alternately with the intra-platform shoal facies association (Fig. 4). It occupies most of the proportion at the lower part of the Lianglitage Formation and is also greater in thickness than the intra-platform shoal deposits at the middle and upper parts of the formation. GR is medium to high in value and shows zigzag pattern in the curve (Fig. 4).

Interpretation Fenestra structure is the product of periodic subaerial exposure at an algae-rich tidal flat environment, which is additionally supported by biding structures and horizontal beddings (Fig. 3k–l). Most of the peloids have round or ellipsoidal shapes and dark colors, which are due to the rich organic matter in micrite (Fig. 3j). Fossils are rare, which show that the sedimentary environment is restricted in water circulation and only suitable for cyanobacteria. These characteristics indicate that the facies association is deposited in restricted lagoon and tidal flat environments.

Facies distribution in sequence stratigraphic framework

Sequence stratigraphy

According to the stratigraphic distribution and facies development patterns displayed on drilling wells and seismic profiles, we analyzed the deposition trend of the facies associations in

the Lianglitage Formation and divided the formation into three sequences (SQ1, SQ2, and SQ3 from bottom to top, respectively, Fig. 4) combined with previous studies on sequence stratigraphy of the Lianglitage Formation in the Tazhong Uplift. Stratigraphic correlation shows that SQ1 at the bottom is not developed in some wells located in the west of No.1 fault zone. The TSTs of SQ1 and SQ2 are characterized by restricted lagoon and tidal flat facies association and a small proportion of shoal deposits, reflecting that the accommodation space increases and the sedimentation rate is generally low. Clay-rich lagoon deposits are formed in MFS, marked by high-value GR logging, and thus are stable in lateral correlation. The HSTs of SQ1 and SQ2 are characterized by multiple cycles of reef-shoal and lagoon deposits, and the thickness of cycles and the proportion of reef-shoal within the cycle tend to increase upward, reflecting that the sedimentation rate exceeds the growth rate of accommodation space, and the reef-shoal has an accretion-progradation trend. The thickness of SQ3 is the smallest, only 50~100m, and the high GR section at the bottom marks the sharp increase of accommodation space, which is mainly caused by sea level rise.

Facies distribution

The vertical and lateral distribution of the different facies associations are displayed in the cross correlation profile of the three wells (Fig. 4). Well TZ88 is composed of three sequences, and wells TZ86 and TZ49 (in the north) are only composed of the upper two sequences (SQ2 and SQ3). SQ1 in well TZ88 was dominated by lagoon deposits and inter-bedded with minor shoal deposits at the upper part of the HST. SQ2 display a distinct lateral variation between platform margin facies (TZ88) and the platform-interior (TZ49). TZ88 comprises the thickest interval of SQ2, characterized by thick-bedded shoals and a reef-shoal complex, while TZ86 was dominated by thick shoal cycles. SQ2 in TZ49 was mainly composed of platform-interior shoal and lagoon deposits. SQ2 in TZ88 and TZ86 recorded higher environmental energy than that in TZ49. SQ3 in TZ88, TZ86, and TZ49 are small in thickness and are largely composed of argillaceous limestones, interpreted as a platform-interior lagoon environment, which was formed during a rapid increase in accommodation space. Sand shoal deposits are small in thickness as is shown in wells TZ86 and TZ88 despite that both wells are located at the platform margin.

Diagenesis

Diagenetic features

Based on the observation of cores and thin sections, we identified various diagenetic events of the Lianglitage Formation and divided them into four categories: compaction, cementation, dissolution, and structural fracture.

Compaction

The Lianglitage Formation experienced intense compaction. Many rocks develop stylolites, which are generally attributed to mineral dissolution under physical compaction (Fig. 5a–c). In reef-shoal deposits, many particles are linear contacted, and some peloids are obviously distorted and deformed (Fig. 3a, e), which indicate strong physical compaction before extensive cementation.

Cementation

The cement of the Lianglitage Formation is dominated by sparry calcites, which are divided into the five types according to the morphology, crystal structure, and cathodoluminescence.

(1) Isopachous fibrous calcite cements (IFC). They are cloudy and unclean under plane polarized light and show dark color in cathodoluminescence (Fig. 5d, e). They commonly grow around the intraclasts and ooids of Lf1 and Lf2 and in the cavity of fossil bodies of Lf3, dissolved pore, and bird's-eye pores of Lf8 and Lf9. In some samples, these cements were observed filling a major proportion of interparticle pores and biological cavities.
(2) Fine equant calcite cements (FEC). These cements are mostly clean and bright under plane polarized light and fill the interparticle pores of Lf1 and Lf2 (Fig. 5d–f). They are also common in densely distributed narrow fractures and intraparticle pores in Lf1 and Lf2 (Figs. 5l, 6a–b).
(3) Bladed calcite cements (BdC). They mainly appear in the biological cavities and large inter-bioclast pores and completely fill these large pores (Fig. 5g–i).
(4) Blocky calcite cements (BkC). They are mainly found filling in various vugs with clean and bright characteristics under plane polarized light. The cements show dark red and orange color under cathodoluminescence with banded characteristics distinguished by different colors (Figs. 5c–f, h–i, 6).
(5) Coarse clusters calcite cements (CCC). This kind of cements is found in wide vertical fractures, and residual bitumen occurs between calcite crystals (Fig. 5j–l). Many crystals are rich in inclusions.

Dissolution

Some dissolution features are related to rock fabric, which are mostly the dissolution of ooids and bioclasts, while others have nothing to do with rock fabric. As a result, various dissolution pores are formed.

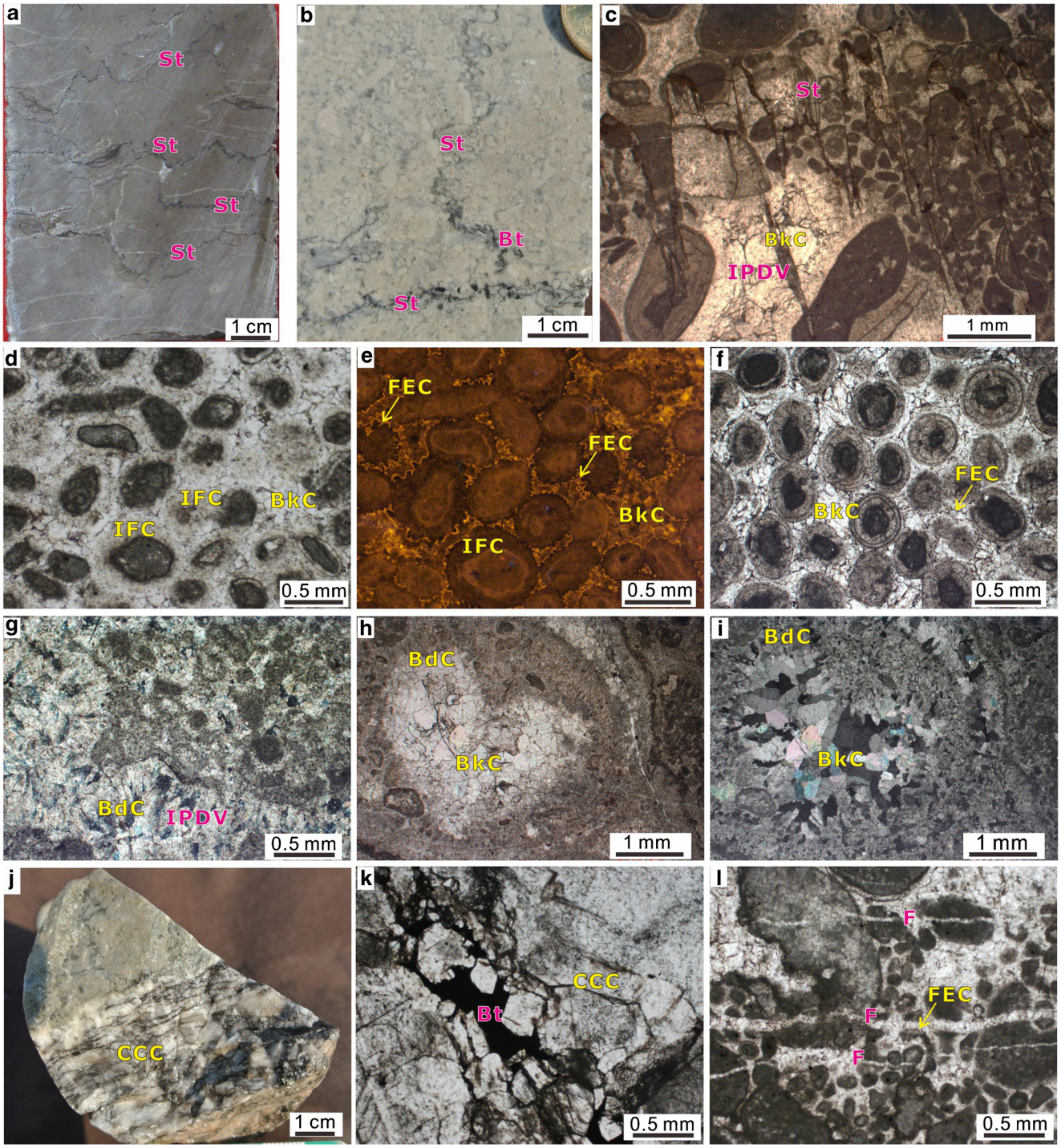

Fig. 5 Diagenetic features of the Lianglitage Formation in the Northwest of Tazhong area. **a** Stylolites in bioclast and peloid wackestone to packstone (Lf6). Platform-interior sand shoal deposits, TZ49, 6279.7 m. **b** Stylolites in ooid grainstone (Lf1), note the bitumen along the stylolites. Platform margin shoal deposits, TZ86, 6271.2 m. **c** Stylolites in ooid and peloid grainstone (Lf2), note the stylolite cut the BkC. TZ85, 6442.6 m, PPL. **d** IFC, FEC, and BkC cements in ooid grainstone (Lf1) and their cathodoluminescence photo (**e**). Platform margin shoal deposits, TZ85, 6443.2 m, PPL. **f** FEC and BkC cements in ooid grainstone (Lf1). Platform margin shoal deposits, TZ85, 6580.2 m, PPL. **g** BdC cement in an interparticle dissolution vug (IPDV) in bioclast and peloid grainstone (Lf3). Platform margin shoal deposits, TZ85, 6443.9 m, XPL. **h** BdC and BkC cements in a dissolution vug in bioclast and peloid grainstone (Lf3). TZ85, 6444.1 m, PPL. **i** The XPL view of **h**. **j** High-angle wide fracture which is filled by CCC. TZ86, 6278.7 m. **k** Bitumen (Bt) filled the space between CCC, TZ86, 6278.7 m; dense narrow fractures developed in peloid grainstone are filled by FEC. Platform margin shoal deposits, TZ86, 6278.7 m

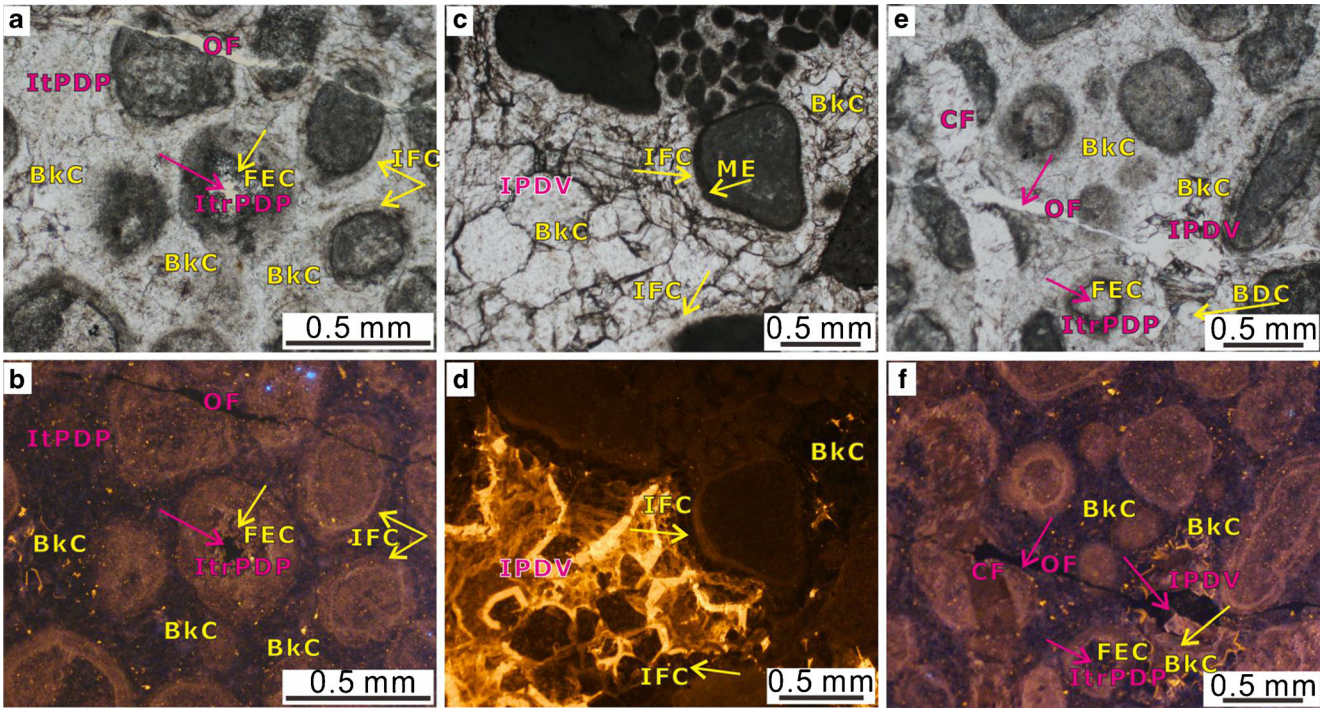

Fig. 6 Dissolution and cementation features of the Lianglitage Formation in the Northwest of Tazhong Uplift. **a** IFC and BkC cements in interparticle dissolution pores (ItPDP) and FEC cements in intraparticle dissolution pores. A narrow open fracture (OF) is unfilled. Platform margin shoal deposits, TZ86, 6275.9 m. **b** The cathodoluminescence of **a**. **c** IFC and BkC cements in dissolution vug, platform margin shoal deposits, TZ86, 6278.7 m. **d** the cathodoluminescence of **c**. **e** A narrow open fracture (OF) cut an interparticle dissolution vug (IPDV) and a filled wide fracture (CF) which is filled by BkC cement. Platform margin shoal deposits, TZ86, 6277.5 m

(1) Birds'-eye pores of fenestra pores. They developed in tidal flat deposits (Lf8 and Lf9) and were related to the binding structure. They showed dissolved pores of different sizes, which developed from 0.1 to 2 mm and distributed along the lamina (Fig. 3k–l). Most fenestra pores are filled by IFC and BkC.
(2) Intraparticle dissolution. It mainly occurs in ooids and bioclasts (Lf1 and Lf2). FEC and BkC filling are common in dissolved pores, and only a small proportion of residual pores are preserved (Fig. 6a–b).
(3) Interparticle dissolution. It occurs in grainstones (Lf1 and Lf2), and the dissolved pores are mainly millimeter-sized and round. Most of the pores are filled with BkC, while a small part is unfilled to form isolated dissolved pores and small vugs (Figs. 5c, 6c–f).
(4) Stylolite. In grainstones, stylolites are serrated and narrow (Fig. 5b). Under the microscope, partial dissolution of the ooids or other grains can be observed, and some stylolites pass through BkC (Fig. 5c). The stylolites developed in micrite limestone are much wider than in grainstones, and residual clay is distributed along the stylolites in micrite-rich limestones (Fig. 5a).
(5) Dissolutions along fractures. This dissolution usually forms large linearly distributed vugs and caves (Figs. 6f, 10e, g, h), in which CCC and occasional fluorite were precipitated.

Tectonic fractures

Fractures are very common in the Lianglitage Formation. The fractures observed in cores mainly include high-angle wide fractures and low-angle narrow fractures. Bitumen and CCC are common in high-angle wide fractures (Fig. 5j–k). The low-angle narrow fractures show reticular shape and/or are densely arranged. Intersecting micro-fractures were frequently observed in thin sections (Fig. 6e–f). The fractures formed earlier are fully filled by BkC and relatively wide (about 0.05mm) and are cut by narrow fractures which are mostly unfilled.

Diagenesis sequence

According to the combination relationship and distribution pattern of various diagenetic characteristics observed by microscope and cathodoluminescence, the diagenetic sequence of the Lianglitage Formation in northwestern Tazhong Uplift is divided into syndepositional submarine diagenetic stage, penecontemporaneous diagenetic stage, and buried diagenetic stage (Fig. 7). The buried diagenetic stage is further divided into two substages.

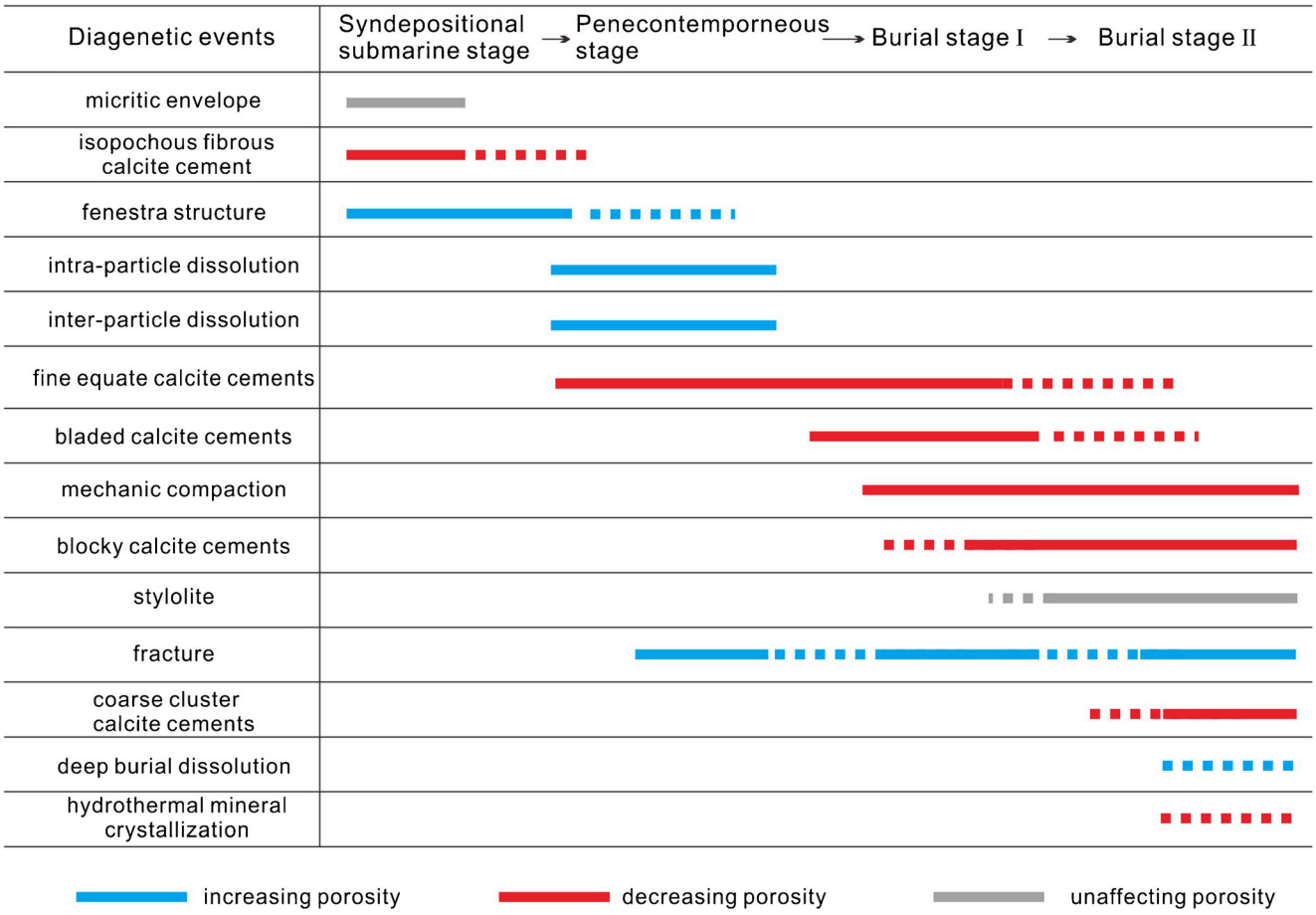

Fig. 7 Diagenetic events and diagenesis stages of the Lianglitage Formation, NW Tazhong Uplift

Syndepositional submarine diagenetic stage

The submarine diagenetic stage occurred on the seafloor during deposition. In the high-energy shoal deposits, the precipitation of high-magnesium calcites and aragonites in the pores between grains characterize this stage; as a result, the IFC and BC were formed. In lagoon with low water energy, micritization occurs at the outer surface of grains, and thin micritic envelops were formed. In tidal flat environment, this diagenetic stage is mainly characterized by the formation of bird's-eye or fenestrae in binding laminations.

Penecontemporaneous diagenetic stage

Penecontemporaneous diagenetic stage occurred shortly after deposition. Due to the slight drop of sea level or/and slight tectonic uplift occurred after the deposition of the Lianglitage Formation, the deposits were separated from seawater environment and thus affected by the meteoric water lens. This tectonic movement is recorded more clearly in the strata in the eastern part of Tazhong area. The high lands formed by the reef and shoal deposits at the platform margin is exposed and leached, which is characterized by high-angle dissolution fractures and caves(Zhu et al. 2017). In the study area, it is mainly identified by the dissolution of grains deposited in sand shoals on the platform margin.

Buried diagenetic stage

Combined with the tectonic evolution history of the study area, it can be divided into two substages.

Burial stage I occurred after penecontemporaneous diagenetic stage, from Late Ordovician to Permian, that is, from Late Caledonian to Hercynian. During this substage, most porosity values were continuously cemented and destroyed. Stylolites also began to form at this substage. The precipitation of cements mainly derived from sealed seawater, so the cathodoluminescence is consistent with the cements which were precipitated during the syndepositional submarine diagenetic stage. In the late Hercynian period, that is, Carboniferous-Permian, the Tazhong area was generally subjected to tectonic uplift (Lin et al. 2012b), forming strike-slip faults with NE orientation, accompanied by a large number of fractures. Magmatism and associated hydrothermal processes also occurred during this period. Fluorites filled in the cave of

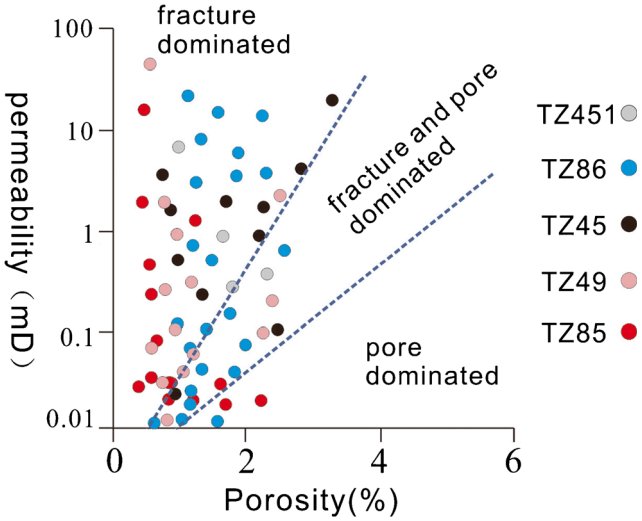

Fig. 8 Distribution of permeability and porosity of the Lianglitage Formation, NW Tazhong Uplift

Tazhong 45 well are generally considered as a direct evidence of hydrothermal activity (Han et al. 2011; Wang et al. 2004).

Burial stage II occurred since Mesozoic, and the Lianglitage Formation was continued to be deeply buried. During this period, pores and fractures are continuously filled by calcite cements. The filling calcite cements are mostly BkC, which shows clearly distinguished zones alternating from dark red to orange yellow under cathodoluminescence. The pressure-soluble stylolites continue to develop. Besides the dissolution of carbonate grains, the dissolution of cements formed prior to this substage, and the precipitation of BkC near the stylolites are also observed.

Reservoir characteristics

Porosity and permeability

Based on the measured porosity and permeability of 76 core samples from 5 wells in the study area, the Lianglitage reservoirs in northwestern Tazhong Uplift generally have low porosity and permeability (Fig. 8). Nearly 1/3 samples have porosity values lower than 1%, nearly 1/2 samples have porosity values of 1~2%, about 1/5 samples have porosity values of 2~3%, and only 1.5% samples have a porosity of over 3%. The permeability of most samples is <1mD, the permeability of 22.5% samples ranges from 1 to 10 mD, and the permeability of about 9% samples is greater than 10 mD.

On the cross-plot of porosity and permeability (Fig. 9), most of the points are distributed near the longitudinal axis (permeability). This reflects that the porosity is generally low, but the permeability changes greatly, and some reservoirs with lower porosity also have high permeability. According to the scatter distribution range of permeability and porosity, reservoirs are divided into three types. (1) Fracture-dominant type. They have low porosity but high permeability. The scattered points are distributed in an area very close to the longitudinal axis. (2) Fracture- and pore-dominant type. They have moderate porosity, and with the increase of porosity, the permeability increases accordingly. Scattered points of this type are distributed in a small area in the middle part of the plot. (3) Pore-dominant type. They have extremely low permeability and medium-low porosity.

Reservoir space

The reservoir space of the Lianglitage Formation in the study area includes fractures, dissolution vugs, karst caves, interparticle pores, and interparticle dissolution pores. The primary fabric-related pores in grainstones are mostly filled with calcite cements.

Dissolution vugs and caves

The effective porosity of pore-type reservoir in the Lianglitage Formation is mainly dissolution pores. A small number of millimeter-sized dissolved vugs are present in the cores, most of which are partially filled with calcite cements, and a small proportion of them still retain effective (Fig. 10a). Microscopically, these pores are mostly developed in Lf1, Lf2 (Figs. 5c, g–i, 6c–f) and Lf9 (Fig. 3k–l). In Lf1, a small proportion of ooids are

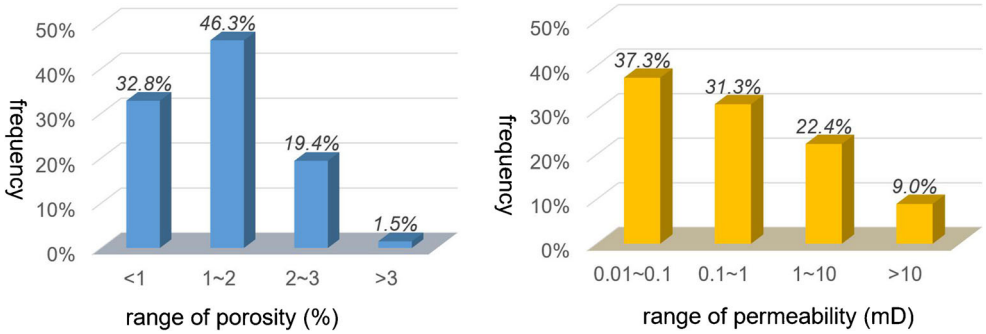

Fig. 9 Permeability and porosity of the Lianglitage Formation, NW Tazhong Uplift

dissolved, forming intraparticle dissolved pores or ooid-moldic pores (Fig. 6a–b). This kind of reservoir is mainly distributed in layers, which is closely related to sand shoals. The other is caves found in cores and drilling, which are closely related to fractures (Fig. 10b–h). The leakage of drilling fluid occurred in well TZ86 at 6288~6289.48 m, and the total amount of lost drilling fluid reaches up to 112.95 m^3. After acidizing, the daily oil production and gas production of related intervals are 42.3 m^3 and 87,000 m^3, respectively. TZ45 developed four large caves bearing intervals at 6095~6099 m, and the fillings in the caves include calcite, fluorite, and clay. There are approximately 140 vugs and caves with diameters of several millimeter to several centimeter in well TZ45 at 6099~6108 m, and the space is partially filled with calcite and quartz. These reservoir beds yielded a production of 300 m^3 oil and 112,000 m^3 gas per day.

Fractures

Fractures are very common in cores and are divided into high-angle fractures and low-angle fractures.

High-angle fractures Densely distributed high-angle fractures are generally straight and narrow, less than 1mm (Fig. 10a–b). This kind of fractures vertically extends for long distance, and residual bitumen can be seen in the fractures, indicating the passing oil and gas activity (Fig. 10a–b). Some high-angle fractures are curved, and the width of fractures vary from 1mm to several centimeter. This kind of fracture does not vertically extend long distance, but the accompanying dissolution and cementation filling are conspicuous (Fig. 10d–e, g, h). Small beaded vugs and caves and CCC occur along the fractures. Many reticular high-angle fractures develop at the middle part of the Lianglitage Formation in well TZ49 at 6187~6196 m, which are mostly filled with bitumen and clay.

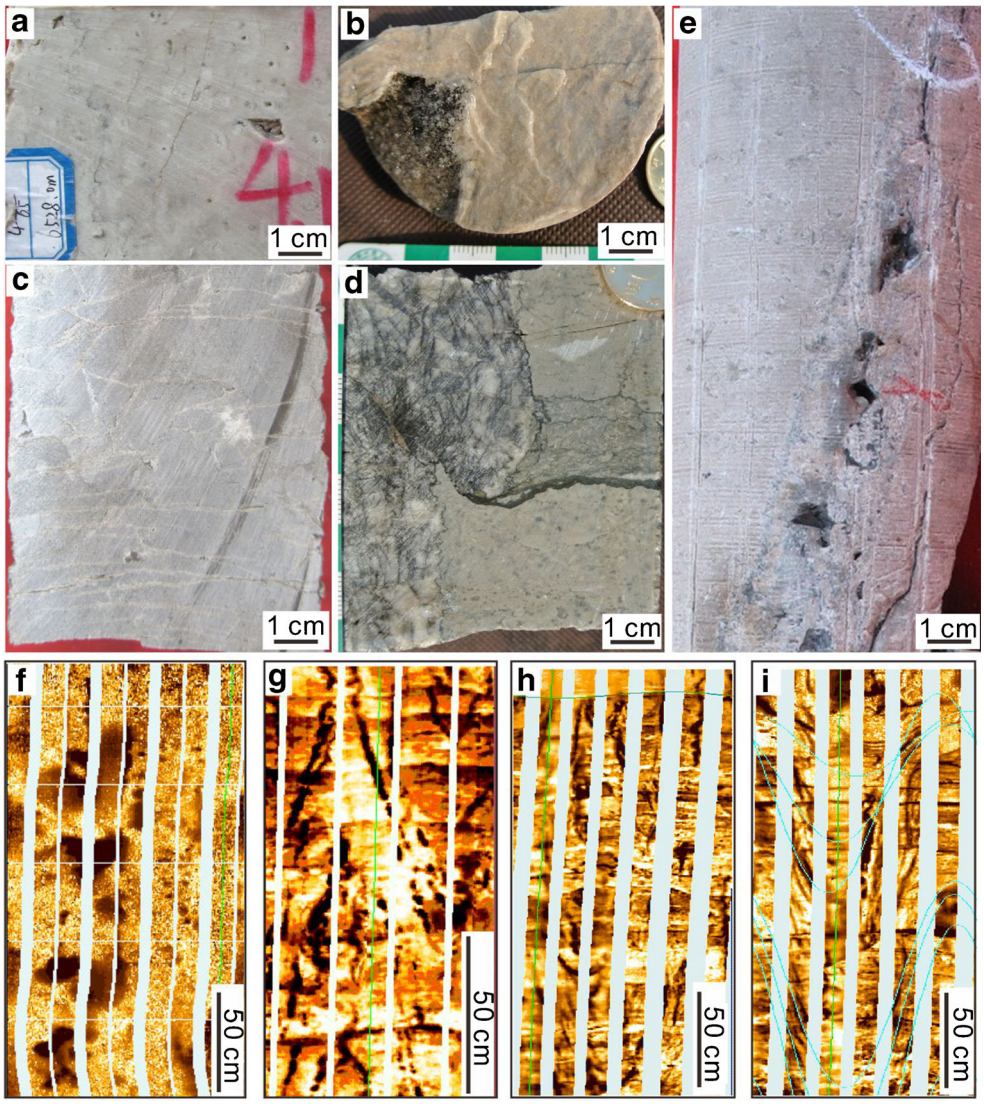

Fig. 10 Characteristics of reservoirs in the Lianglitage Formation in the Northwest of Tazhong Uplift. **a** Dissolution vugs in grainstone. Platform margin reef-shoal deposits, TZ85, 6528.8 m. **b** Dissolution cave and coarse calcite cements. Platform margin shoal deposits, TZ86, 6275.8 m. **c** Multiple fractures and dissolution vugs in peloid packstone. Platform-interior shoal deposits, TZ49, 6283 m. **d** Wide fracture filled with coarse-crystalline calcite. Platform margin shoal deposits, TZ86, 6270.5 m. **e** Fractures and associated dissolution vugs and beaded caves. Platform margin shoal deposits, TZ86, 6272 m. **f** Beaded-distributed vugs and caves. TZ45, 6097~6099 m. **g** Conjugated high-angle fractures and associated dissolution vugs. TZ86, 6305~6306 m. **h** Goose-lined fractures and associated dissolution vugs. ZG18, 6214~6216 m. **i** Dense goose-lined fractures. ZG18, 6206~6208 m

High-angle fractures are developed at the middle to upper parts of the Lianglitage Formation in well TZ86, accompanied by beaded karst caves, which are filled with bitumen and calcite cements, forming good reservoir beds.

Low-angle fractures Most low-angle fractures are densely arranged in cores, and the distance between adjacent fractures ranges from several millimeter to several centimeter. Some fractures show arch shapes, and some adjacent fractures are joined by high-angle fractures which do not extend far (Fig. 10c). Most of these fractures are filled with calcite cements, and dissolution vugs associated with fractures can also be seen.

There are about 100 near-horizontal low-angle fractures in well TZ45 at 6054~6068 m, most of which are filled with calcite. The cores at the lower part of the Lianglitage Formation in well TZ49 at 6280~6288m have many nearly horizontal fractures, the vertical development density can reach 1~2 per centimeter, and most of them are partially filled with calcite cement.

Distribution of reservoir beds

According to the interpretation results of reservoir by well logging data, the good reservoir beds mainly develop at the middle-upper part of the Lianglitage Formation (Fig. 11). The ratio of the total thickness of reservoir beds to that of the Lianglitage Formation ranges from 10 to 40%. The ratios of drilling wells near No.1 fault zone on platform margin are higher, such as 40% in TZ86 and 30% in TZ88. The ratios of drilling wells inside the platform are low, such as 19% in TZ49 and 12% in TZ63. The thickness of a single set of reservoirs beds is usually distributed between 5 and 10 m, and only a few reservoirs beds are thicker than 20 m, which are preserved in platform margin shoal deposits. The porosity of the reservoir is generally 1~3%, and only a few locally distributed intervals have porosity greater than 3%.

Well-developed reservoir beds mainly show stronger amplitude and are mainly distributed near the platform margin and fault zone, as is shown in the seismic attribute map (Fig. 12). Especially, drilling wells with high productivity mainly locate at the intersection areas of faults, at the area where the strike orientation of the fault changes and at the end of faults.

Discussion

Controlling factors on reservoirs

Deposition and diagenesis

Reefs and shoal deposits generally have good primary porosity, and the reservoir space is dominated by interparticle pores.

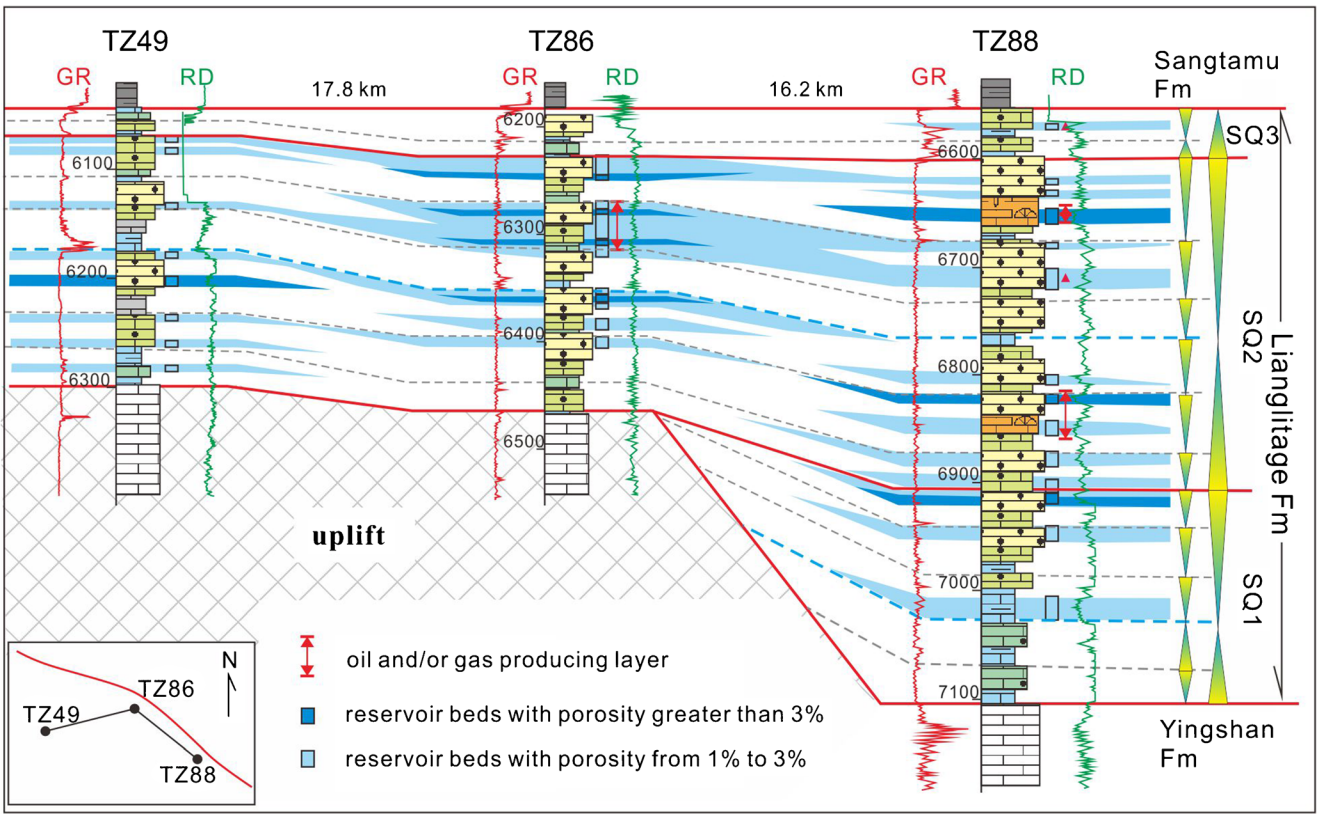

Fig. 11 The distribution of reservoir beds between drilling wells in the Lianglitage Formation in the Northwest of the Tazhong Uplift

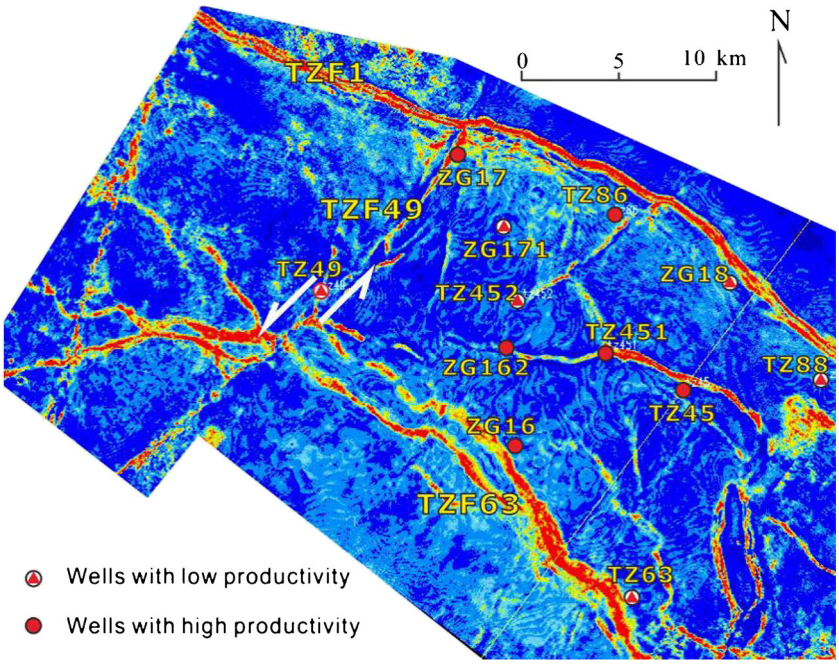

Fig. 12 3-D seismic attribution map showing the location of high and low productivity wells relative to faults

After compaction and cementation, however, pores in these reservoir beds are intensely destructed or filled. Although the early-formed fenestra pores of tidal flat deposit are well developed, the matrix pores are almost destroyed due to continuous cementation. The matrix pores of other lithofacies are generally very low. In penecontemporaneous diagenetic stage, the ooids and skeletal grains in reef and shoal deposits were partially dissolved by meteoric water, forming intraparticle pores, interparticle dissolved pores, vugs, and caves. This dissolution mainly occurs at the top of reef-shoal complex, forming quasi-layered reservoir beds, which are scattered in the strata of the Lianglitage Formation in the study area (Gao et al. 2016). Only in very few drilling wells, large karst caves are formed (Gao et al. 2013; Shen et al. 2010; Zhang et al. 2011; Zheng et al. 2015). According to the distribution of facies association, the proportion and horizontal distribution of reef-shoal complex in the platform margin area are better developed than those in the platform-interior area, so the reservoir beds in the platform margin are better in vertical continuity and horizontal stability than those in platform-interior area. Compared with the Lianglitage Formation reservoir in eastern well area of Tazhong area, penecontemporaneous diagenesis has weaker dissolution and transformation of reservoirs in the study area.

There are also research results that attribute these porous reservoirs to dissolution in deep buried environment (Han et al. 2011; Wang and Lü 2004; Wang et al. 2004). However, based on the microscopic characteristics of the fillings in the pores of the reef-shoal lithofacies, we found that the cements precipitated from contemporaneous seawater are preserved in these pores, and their cathodoluminescence is consistent with the FC, BC, and FEC cements filling between particles. This indicates the early formation of these vugs and caves. It is the degree of filling during burial diagenetic stage that determines the quality of the reservoir beds. From the core and thin section observation, most reef-shoal deposits are strongly cemented during burial stage, resulting in rather low porosity. Nevertheless, these pores are very important for the formation of reservoir beds.

In the stage of burial diagenesis, especially in the end of Permian, the tectonic movement was accompanied by magma intrusion, which had marked influence on the reservoir quality. Thick igneous rocks were found in some wells in the study area, and some caves were found filling with hydrothermal minerals. In addition, organic acids formed during the maturation of organic matter (Hu et al. 2009) and acidic fluids formed by TSR (Sun et al. 2007) are also considered as factors for reservoir improvement. We do not deny that this kind of acidic fluid has potential significance for reservoir improvement, but we are more inclined to this understanding that the amount of fluid needed for large-scale dissolution is insufficient; in addition, local dissolution will inevitably be accompanied by mineral precipitation and pore filling from the perspective of material balance in such a deep-buried environment (Ehrenberg et al. 2012; Li et al. 2010b; Zhang et al. 2017). Based on the characteristics of pores and fillings of Lianglitage Formation reservoirs in the study area, we emphasize that the reservoir beds mainly experienced pore preservation or pore destruction during burial diagenesis, rather than the formation of new pores.

Faults and fractures

In the study area, almost all the reservoir beds discovered by drilling wells are related to faults and associated fractures. They are formed into two stages of tectonic movement. Multistage tectonic movements experienced in the study area, especially those occurred in the end of Ordovician and Silurian-Devonian, are the most important to improve the reservoir quality.

At the end of Ordovician, with the subduction of the ancient oceans at the basin margin, a series of thrust faults with NW-SE strike were formed in Tazhong area (Li et al. 2010a). Intense uplift was formed in the southeast of Tazhong area, and the Lianglitage Formation was completely denuded in those areas (Gao et al. 2018). There is also an obvious uplift in the study area. As a result, horizontal fractures were formed at the top of the uplift where the tectonic stress is released, and high-angle fractures were formed at the upper wall of thrust faults. This development mechanism is similar to the settings near Tazhong No.10 fault zone at the center part of Tazhong area (Deng et al. 2018; Yang et al. 2018; Zhang et al. 2016a).

During Silurian-Devonian, a series of strike-slip faults with NE strike were formed in Tazhong area, which can be further divided into main faults, terminal feather-like faults, and pull-apart grabens (Li et al. 2010a). New fracture systems associated with these faults are mainly tensile fractures. Fault-karst reservoirs have been found in Shunbei area in the northeast of the study area and near Tazhong No.10 fault zone (Deng et al. 2018; Jiao 2018). More than 90% of high-yielding wells are distributed along strike-slip fault zones, and oil and gas are more enriched at the top of the large-scale strike-slip faults and their branch faults and at the tension and torsion parts of the strike-slip faults (Han et al. 2019; Zhang et al. 2016b). From the view of rock mechanics, it is proved that brittle mechanical deformation of strata caused by strike-slip faults is an important factor for reservoir improvement. Strike-slip faults spreading in the northeast of the study area also play an important role in improving the reservoir quality.

Implications for deep-burial limestone hydrocarbon exploration

Based on the study of sedimentation and diagenesis of Lianglitage Formation reservoir in the northwest of Tazhong area, we sum up the implications for oil and gas exploration of deep buried limestone reservoir in the study area.

First, it is necessary to focus on detailed facies analysis and clarify the stratigraphic and spatial distribution of reefs and shoal within the sequence stratigraphic framework. Then, combined with 3-D seismic data, paleogeomorphology reconstruction is important to identify the area where thick reef and shoal deposits were generated.

At platform margin area, reef-beach facies develop better and early karstification during penecontemporaneous diagenetic stage plays a key role in the improvement of reservoir quality. Therefore, it is important to find where karst caves and fractures are superimposed. The reservoirs developed at platform margin are close to the source rocks formed in slope and basin environment resulting in a good accumulation condition.

At the platform-interior area, the shoal deposits are small in thickness and scattered distributed. The reservoirs are slightly improved by penecontemporaneous diagenesis, coupled with strong cementation in the later burial diagenesis stage, resulting in low-porosity reservoir beds and high risk of hydrocarbon exploration. Faults and fractures are crucial to the formation of effective reservoir beds.

Conclusions

The Lianglitage Formation in the northwest of Tazhong area is mainly composed of nine lithofacies that are deposited from platform margin reef-shoal, platform-interior shoal, and restricted lagoon-tidal flat environments. In the high systems tracts of sequence, reef and shoal deposits are thicker and distributed more continuously.

The Lianglitage Formation in the study area has experienced syndepositional submarine diagenesis, penecontemporaneous diagenesis, and burial diagenesis, during which the reservoir beds were subjected to continuous cementation. Penecontemporaneous diagenesis and tectonic movement during burial diagenesis are constructive to the formation of reservoir beds.

The reservoir space of the Lianglitage Formation in the study area mainly includes fractures and dissolution vugs and caves. Reef and shoal deposits are the material basis of favorable reservoirs, and the discovered favorable reservoirs are mainly formed by the dissolution of meteoric water in penecontemporaneous diagenesis. In the burial stage, the porosity was destroyed by cementation, but the fractures and associated fractures formed in the late Ordovician and Silurian-Devonian played an important role in the formation and improvement of the reservoir.

For hydrocarbon exploration of deep limestone reservoir, attention should be paid to find reservoir beds with caves and fractures in reef and shoal facies; with regard to those areas where deposits are poor in primary porosity, more emphasis should be placed on the prediction of fracture reservoir beds.

Acknowledgements This work was sponsored by the National Natural Science Foundation of China (Nos. 41502104 and 41130422), the Open Fund of Key Laboratory of Exploration Technologies for Oil and Gas Resources (Yangtze University), Ministry of Education (K-2018-06), and the National Key Basic Research Project (973 Project) (No. 2011CB201100-03). We would like to thank PetroChina Tarim Oilfield

Company for data support. We also thank Dr. Ngia Roger Ngong for carefully proofreading the manuscript.

Declarations

Conflict of interest The authors declare that they have no competing interests.

References

Chen X, Zhao ZJ, Zhang BM, Liu YH (2009) Delicata sedimentary model to Lianglitage Formation of Upper Ordovician in the northern margin of isolated platform in the center of Tarim Basin. Acta Sedimentol Sin 27:1002–1011 (in Chinese with English abstract)

Deng X et al (2018) Origin, development and features of the "fault-dissolved body" reservoir formed in burial stage: a case study of Upper Ordovician Lianglitage Formation in Tarim Basin, Northwest China. Mar Orig Pet Geol 23:47–55 (in Chinese with English abstract)

Dunham RJ (1962) Classification of carbonate rocks according to depositional textures. In: Ham W (ed) Classification of Carbonate Rocks–A Symposium. AAPG Memoir, pp 108-121

Ehrenberg SN, Walderhaug O, Bjørlykke K (2012) Carbonate porosity creation by mesogenetic dissolution: reality or illusion? AAPG Bull 96:217–233. https://doi.org/10.1306/05031110187

Embry AF, Klovan JE (1971) A Late Devonian reef tract on northeastern Banks Island, NWT. Bull Can Petrol Geol 19:730–781

Gao D et al (2013) Microfacies of late Ordovician Lianglitage Formation and their control on favorable reservoir in Tazhong area. Earth Sci 38:819–831 (in Chinese with English abstract)

Gao D, Lin C, Yang H, Zuo F, Cai Z, Zhang L, Liu J, Li H (2014) Microfacies and depositional environments of the Late Ordovician Lianglitage Formation at the Tazhong Uplift in the Tarim Basin of Northwest China. J Asian Earth Sci 83:1–12. https://doi.org/10.1016/j.jseaes.2014.01.002

Gao D, Lin C, Hu M, Huang L (2016) Using spectral gamma ray log to recognize high-frequency sequences in carbonate strata: a case study from the Lianglitage Formation from well T1 in Tazhong area, Tarim Basin. Acta Sedimentol Sin 34:707–715 (in Chinese with English abstract)

Gao D, Lin C, Hu M, Yang H, Huang L (2018) Paleokarst of the Lianglitage Formation related to tectonic unconformity at the top of the Ordovician in the eastern Tazhong Uplift, Tarim Basin, NW China. Geol J 53:458–474

Han JF, Sun CH, Yu HF, Ji YG, Zhang ZH, Xu YL (2011) Kinetics of reef-shoal complexes and its restriction to reservoir in Ordovician from Tazhong I fault belt. Acta Petrol Sin 27:845–856 (in Chinese with English abstract)

Han J et al (2019) Reservoir-controlling and accumulation-controlling of strike-slip faults and exploration potential in the platform of Tarim Basin. Acta Pet Sin 40:1296–1310 (in Chinese with English abstract)

He Z, Jin X, Wo Y, Li H, Bai Z, Jiao C, Zhang Z (2016) Hydrocarbon accumulation characteristics and exploration domains of ultra-deep marine carbonates in China. China Pet Explor 21:3–14 (in Chinese with English abstract)

Hu MY, Cai XY, Hu ZG, Qian Y, Xiang J (2009) Deep buried dissolution of Ordovician carbonates in Tazhong area of Tarim Basin. J Oil Gas Technol 31:49–54 (in Chinese with English abstract)

Jia CZ (1997) Tectonic characteristics and petroleum in Tarim Basin of China. Petroleum Industry Press, Beijing (in Chinese)

Jiao F (2018) Significance and prospect of ultra-deep carbonate fault-karst reservoirs in Shunbei area, Tarim Basin. Oil Gas Geol 39:207–216 (in Chinese with English abstract)

Li C, Wang X, Li B (2010a) Paleozoic faulting structure styles of the Tazhong low uplift, Tarim Basin and its mechanism. Acta Geol Sin 84:1727–1734 (in Chinese with English abstract)

Li Z et al (2010b) Buried diagenesis, structurally controlled thermal-fluid process and their effect on Ordovician carbonate reservoirs in Tahe, Tarim Basin. Acta Sedimentol Sin 28:969–979 (in Chinese with English abstract)

Lin C, Yang H, Liu J, Peng L, Cai Z, Yang X, Yang Y (2009) Paleostructural geomorphology of the Paleozoic central uplift belt and its constraint on the development of depositional facies in the Tarim Basin. Sci China Ser D Earth Sci 52:823–834. https://doi.org/10.1007/s11430-009-0061-8

Lin C, Yang H, Liu J, Rui Z, Cai Z, Li S, Yu B (2012a) Sequence architecture and depositional evolution of the Ordovician carbonate platform margins in the Tarim Basin and its response to tectonism and sea-level change. Basin Res 24:559–582. https://doi.org/10.1111/j.1365-2117.2011.00536.x

Lin C, Yang H, Liu J, Rui Z, Cai Z, Zhu Y (2012b) Distribution and erosion of the Paleozoic tectonic unconformities in the Tarim Basin, Northwest China: significance for the evolution of paleo-uplifts and tectonic geography during deformation. J Asian Earth Sci 46:1–19. https://doi.org/10.1016/j.jseaes.2011.10.004

Liu L et al (2009) Paleozoic reservoir beds and their favorableness in Tazhong Areas of Tarim Basin, Northwest China. J Pet Sci Eng 68:1–18. https://doi.org/10.1016/j.petrol.2009.05.014

Liu JQ, Li Z, Han YX, Peng ST (2010) Early diagenesis in high-frequency sequence framework of the Upper Ordovician carbonate platform in Tazhong, Tarim Basin and its influence on reservoir distribution. Acta Petrol Sin 26:3629–3640 (in Chinese with English abstract)

Liu J, Lin C, Li S, Cai Z, Xia S, Fu C, Liu Y (2012) Detrital zircon U-Pb geochronology and its provenance implications on Silurian Tarim basin. J Earth Sci 23:455–475. https://doi.org/10.1007/s12583-012-0268-z

Lü XX, Yang N, Xie QL, Yang HJ (2005) Carbonate reservoirs transformed by deep fluid in Tazhong area. Oil Gas Geol 26:284–289+296 (in Chinese with English abstract)

Lü XX, Yang N, Zhou XY, Yang HJ, Li J (2008) Influence of Ordovician carbonate reservoir beds in Tarim Basin by faulting. Sci China Ser D Earth Sci 51:53–60. https://doi.org/10.1007/s11430-008-6016-7

Lü X, Han J, Wang X, Jiao W, Yu H, Hua X, Zhang H, Zhao Y (2012) Hydrocarbon distribution pattern in the Upper Ordovician carbonate reservoirs and its main controlling factors in the west part of northern slope of central Tarim Basin, NW China. Energy Explor Exploit 30:775–792

Ma X, Hou J, Hu X, Liu Y, Qi D, Ma X, Zou J (2013) Framework of fault-controlled meteoric palaeokarst Ordovician reservoirs in Tahe oilfield, Tarim Basin. Geol Rev 59:521–532 (in Chinese with English abstract)

Ma Y, Cai X, Zhao P (2014) Characteristics and formation mechanisms of reef-shoal carbonate reservoirs of Changxing-Feixianguan formations, Yuanba gas field. Acta Pet Sin 35:1001–1011 (in Chinese with English abstract)

Ma Y, He Z, Zhao P, Zhu H, Han J, You D, Zhang J (2019) A new progress in formation mechanism of deep and ultra-deep carbonate reservoir. Acta Pet Sin 42:1415–1425 (in Chinese with English abstract)

Ma Y et al (2020) Mechanisms and exploitation of deep marine petroleum accumulations in China: advances, technological bottlenecks and basic scientific problems. Oil Gas Geol 41:1–19

Moore CH (2001) Carbonate reservoirs: porosity, evolution and diagenesis in a sequence stratigraphic framework, vol 55. Elsevier

Peng L, Liu XP, Lin CS, Liu JY, Yang XF, Wang HP, Li HP (2009) Late Ordovician palaeogeomorphology and its sedimentary facies characteristics in central Tarim uplift. Oil Geophys Prospect 44:767–772 (in Chinese with English abstract)

Qian Y, He Z, Zou Y, Chen Y, You D (2008) The meteoric diagenesis of the Upper Ordovician carbonate rocks occurred in syn-sedimentary karstification in the No.1 belt of northwestern Tazhong, Tarim Basin-taking the well Shun-2 as an example. Earth Sci Front 15: 59–66 (in Chinese with English abstract)

Qian YX et al (2013) An approach to Caledonian unconformities and sequence stratigraphic patterns and distribution of reservoirs of Ordovician carbonate in the western Tazhong area, Tarim Basin. Earth Sci Front 20:260–274 (in Chinese with English abstract)

Qiu H, Yin T, Cao Z, Han J, Huang C, Wei H, Liu Z (2017) Strike-slip fault and Ordovician petroleum exploration in northern slope of Tazhong Uplift, Tarim Basin. Mar Orig Pet Geol 22:44–52 (in Chinese with English abstract)

Qu HZ, Wang ZY, Yang HJ, Zhang YF, Yu HF, Wang X (2013) Karstification of reef-bank facies carbonate rock and its control on pore distribution: a case study of Upper Ordovician Lianglitage Formation in eastern Tazhong area, Tarim Basin, NW China. Pet Explor Dev 40:552–558 (in Chinese with English abstract)

Scholle PA, Ulmer-Scholle DS (2003) A color guide to the petrography of carbonate rocks: grains, textures, porosity, diagenesis, AAPG Memoir 77 vol 77. AAPG

Shen Y, Li Y, Zhao L, Liu Y, Sun Y, Li M (2010) Paleocave as a proxy for calculating uplift amplitude of the Late Ordovician in Central Tarim, Xinjiang, Northwest China. Chin J Geol 45:349–360 (in Chinese with English abstract)

Sun YS, Han J, Zhang LJ, Tan ZJ (2007) Genesis of reef flat body matrix secondary pores in Upper Ordovician in central area of Tarim Basin: A case from Well 62 field of Central Tarim. Pet Explor Dev 34:541–547 (in Chinese with English abstract)

Wang S, Lü X (2004) Features and petroleum significance of Ordovician carbonate reservoir in Tazhong area, Talimu Basin. J Xi'an Shiyou Univ (Nat Sci Ed) 19:72–76 (in Chinese with English abstract)

Wang SM, Jin ZJ, Xie QL (2004) Transforming effect of deep fluids on carbonate reservoirs in the well TZ45 region. Geol Rev 50:543–547 (in Chinese with English abstract)

Wei H, Shi G, Zhu X, Zhang Y, Wang Z (2020) Variation between platform margin and open platform reef-shoal reservoirs of the Lianglitage Formation in the western Tarim Basin. J Southwest Pet Univ (Sci Technol Ed) 42:25–38 (in Chinese with English abstract)

Wu GH, Yang HJ, Qu TL, Li HW, Luo CS, Li BL (2012) The fault system characteristics and its controlling roles on marine carbonate hydrocarbon in the central uplift, Tarim Basin. Acta Pet Sin 28:793–805 (in Chinese with English abstract)

Yan W et al (2019) Sedimentary characteristics of carbonate shoals of Ordovician Lianglitage Formation in Tazhong and Shuntuoguole area, Tarim Basin. J Jilin Univ (Earth Sci Ed) 49:621–636 (in Chinese with English abstract)

Yang HJ, Li Y, Liu S, Li XS, Chen JS, Wang ZY, Dai ZY (2000) Classification and correlation of Middle-Upper Ordovician in Tazhong area and its key understanding. Xinjiang Pet Geol 21: 208–212 (in Chinese with English abstract)

Yang X, Lin C, Yang H, Han J, Liu J, Zhang Y, Peng L, Jing B, Tong J, Wang H, Li H (2010) Depositional architecture of the late Ordovician drowned carbonate platform margin and its responses to sea-level fluctuation in the northern slope of the Tazhong region, Tarim Basin. Pet Sci 7:323–336. https://doi.org/10.1007/s12182-010-0074-0

Yang HJ, Zhu GY, Wang Y, Su J, Zhang BT (2014) The geological characteristics of reservoirs and major controlling factors of hydrocarbon accumulation in the Ordovician of Tazhong area, Tarim Basin. Energy Explor Exploit 32:345–367

Yang Y et al (2018) Characteristic of strike-slip fault and its control effect on the fractured-vuggy carbonate reservoirs in ZG-8 well area. Comput Tech Geophys Geochem Explor 40:425–430 (in Chinese with English abstract)

Zhang Y, Zhang H, Sun C, Ji Y, Han J, Zhang Y (2011) The reef-flat weathering crust karst and its effect on reservoirs in Tazhong area, Tarim Basin. XinJiang Petrol Geol 32:253–256 (in Chinese with English abstract)

Zhang L, Wu G, He S, She Z, Pan Y (2016a) Structural diagenesis in carbonate fault damage zone: a case study of the No.1 fault zone in the Tarim Basin. Acta Petrol Sin 32:922–934 (in Chinese with English abstract)

Zhang Y, Lyu X, Yu H, Jing B, Zhang C, Cai J (2016b) Controlling mechanism of two strike-slip fault groups on the development of the Ordovician karst reservoirs in the Tazhong Uplift, Tarim Basin. Oil Gas Geol 37:663–673 (in Chinese with English abstract)

Zhang H, Cai Z, Qi L, Yun L (2017) Diagenesis and origin of porosity formation of Upper Ordovician carbonate reservoir in northwestern Tazhong condensate field. J Nat Gas Sci Eng 38:139–158. https://doi.org/10.1016/j.jngse.2016.12.008

Zhao ZJ, Zhou XY, Wang ZM, Shen AJ (2007) Distribution of marginal facies and main controlling factors of reservoirs in the Ordovician, the Tarim Basin. Oil Gas Geol 28:738–744 (in Chinese with English abstract)

Zheng J, Wang Z, Yang H, Sun C, Zhang Y, Chen J (2015) Buried karstification period and contribution to reservoirs of Ordovician Yingshan Formation in Tazhong area. Geoscience 29:665–674 (in Chinese with English abstract)

Zhou B, Jia C, Gu J, Li Q, Wu G, Ju Y (2008) Controlling effect of the fractures in Upper Ordovician fractures upon reservoir formation at the platform edge of Tazhong oilfield, the Tarim Basin——an example from the Tazhong-I Slope Break Zone. Oil Gas Geol 29:198–203+209 (in Chinese with English abstract)

Zhu F, Fan T, Gao Z (2010) Sedimentary facies and reservoir characteristics of Lianglitage Formation in west area of Shuntuoguole. Fault-block Oil Gas Field 17:521–524 (in Chinese with English abstract)

Zhu H, Bai X, Wan Y, Ye N, Zhou B, He Y (2017) Carbonate reservoir characteristics and diagenesis in the Lianglitage Formation, Tazhong region, Xinjiang. Sediment Geol Tethyan Geol 37:88–95 (in Chinese with English abstract)

Zou C, Wei G, Xu C, du J, Xie Z, Wang Z, Hou L, Yang C, Li J, Yang W (2014) Geochemistry of the Sinian–Cambrian gas system in the Sichuan Basin, China. Org Geochem 74:13–21. https://doi.org/10.1016/j.orggeochem.2014.03.004

Zuo F, Lin C, Gao D, Zhao J, Xia S, Li H (2014) Sedimentary characteristics and their evolution of Lianglitage Formation in northwestern Tazhong area. Geoscience 28:1008–1016 (in Chinese with English abstract)